Tissue plasminogen activator prevents white matter damage following stroke

Fernando Correa,[1,2,3,4] Maxime Gauberti,[1,2,3] Jérôme Parcq,[1,2,3] Richard Macrez,[1,2,3] Yannick Hommet,[1,2,3] Pauline Obiang,[1,2,3] Miriam Hernangómez,[4] Axel Montagne,[1,2,3] Géraldine Liot,[5] Carmen Guaza,[4] Eric Maubert,[1,2,3] Carine Ali,[1,2,3] Denis Vivien,[1,2,3] and Fabian Docagne[1,2,3]

[1]Institut National de la Santé et de la Recherche Médicale (INSERM), INSERM-U919, Caen Cedex, F-14074 France
[2]Université de Caen Basse-Normandie, Caen Cedex, F-14074 France
[3]Groupement d'Intérêt Public Cyceron, Caen, F-14074 France
[4]Laboratory of Neuroimmunology, Functional and Systems Neurobiology Department, Instituto Cajal, 28002 Madrid, Spain
[5]Centre National de la Recherche Scientifique UMR 146, Institut Curie, 91405 Orsay, France

Tissue plasminogen activator (tPA) is the only available treatment for acute stroke. In addition to its vascular fibrinolytic action, tPA exerts various effects within the brain, ranging from synaptic plasticity to control of cell fate. To date, the influence of tPA in the ischemic brain has only been investigated on neuronal, microglial, and endothelial fate. We addressed the mechanism of action of tPA on oligodendrocyte (OL) survival and on the extent of white matter lesions in stroke. We also investigated the impact of aging on these processes. We observed that, in parallel to reduced levels of tPA in OLs, white matter gets more susceptible to ischemia in old mice. Interestingly, tPA protects murine and human OLs from apoptosis through an unexpected cytokine-like effect by the virtue of its epidermal growth factor–like domain. When injected into aged animals, tPA, although toxic to the gray matter, rescues white matter from ischemia independently of its proteolytic activity. These studies reveal a novel mechanism of action of tPA and unveil OL as a target cell for cytokine effects of tPA in brain diseases. They show overall that tPA protects white matter from stroke-induced lesions, an effect which may contribute to the global benefit of tPA-based stroke treatment.

CORRESPONDENCE
Fabian Docagne:
docagne@cyceron.fr

Abbreviations used: EGF, epidermal growth factor; EGFR, EGF receptor; Erk, extracellular regulated kinase; LBS, lysine binding site; LRP, low-density lipoprotein receptor–related protein; MCAO, middle cerebral artery occlusion; NMDA, *N*-methyl-D-aspartate; OL, oligodendrocyte; PI3K, phosphoinositide 3 kinase; RAP, receptor-associated protein; TFD, trophic factor deprivation; tPA, tissue plasminogen activator.

To date, ∼400 clinical trials concern acute ischemic stroke, of which >270 are considered to be complete (http://www.strokecenter.org/trials). Although >1,000 molecules were shown to display neuroprotective effects in animal models of stroke, none of them has proved efficient when submitted to clinical trials (O'Collins et al., 2006). This admission of failure illustrates the current difficulty to translate animal investigations into successful treatments for human stroke therapy. Such failure likely results from the way animal studies have been designed and how results are interpreted (Young et al., 2007). In fact, clear discrepancies exist between experimental studies and the actual clinical situation.

For instance, most of the experimental studies are conducted in young animals, although stroke generally occurs in aged patients, making aging the principal risk factor for this disease. Nevertheless, therapeutic strategies that protect young tissues are not necessarily efficient in older subjects. It is thus crucial to take the age factor into account in animal studies.

Also, although white matter tissues are affected in most cases of stroke in human, accounting for half of the lesion volume (Ho et al., 2005), they have largely been neglected in most animal studies (Arai and Lo, 2009). Because gray matter and white matter are very different in their structure and cellular content, the mechanisms leading to their degeneration after cerebral ischemia are distinct from each other. Thus, drugs which protect gray matter are not necessarily efficient in saving white matter. This could explain, in part, the failure of stroke clinical trials (Dewar et al., 1999). For this reason,

F. Correa and M. Gauberti contributed equally to this paper.
F. Correa's present address is Dept. of Medical Biochemistry and Cell Biology, Institute for Biomedicine, Sahlgrenska Academy, University of Gothenburg, Gothenburg, Sweden.

The Rockefeller University Press $30.00
J. Exp. Med. Vol. 208 No. 6 1229-1242
www.jem.org/cgi/doi/10.1084/jem.20101880

The Journal of Experimental Medicine

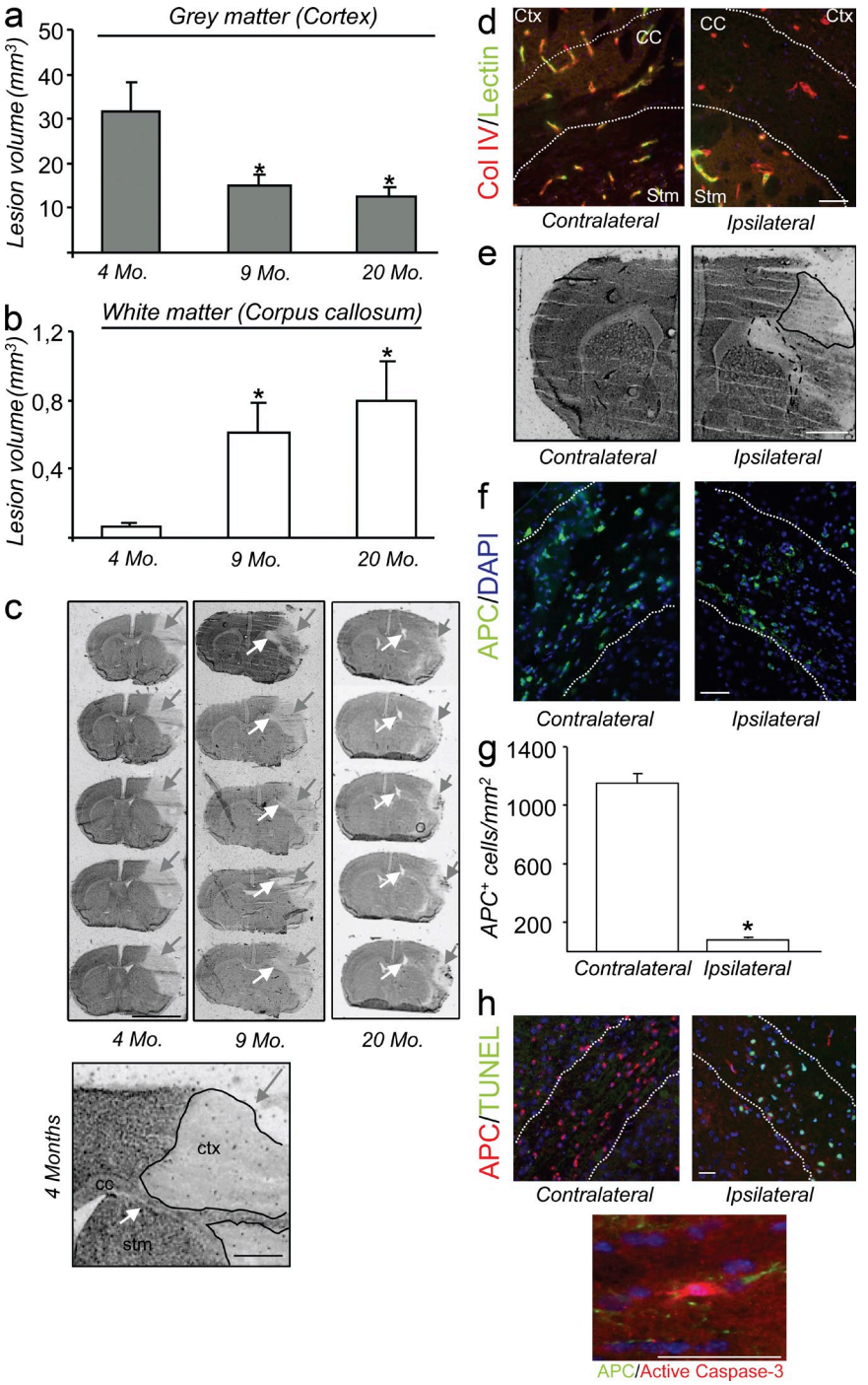

Figure 1. Aging differentially influences gray and white matter susceptibility to stroke. (a and b) C57/BL6 mice (4, 9, and 20 mo old) were subjected to permanent MCAO. Tissue sections were stained with thionin and lesion volumes were quantified in gray matter (cortex; a) and white matter (corpus callosum; b) 24 h after the onset of ischemia (mean + SEM; n = 5–11). *, significantly ($P < 0.05$) different from 4-mo-old mice, Mann-Whitney U test.(c) Representative thionin-stained tissue sections from mice subjected to MCAO at different ages. White arrows show white matter lesions, and gray arrows show gray matter lesions. Bar, 1 cm. The bottom shows gray matter lesion (gray arrow) in 4-mo animals at a higher magnification. Note the absence of lesion in the white matter (white arrow). Stm, striatum; cc, corpus callosum; ctx, cortex (n = 5–11). Bar (bottom), 0.25 cm. (d) Representative image (n = 3) of colocalization of collagen IV immunostaining (red) with lectin-FITC (green) in the contralateral and ipsilateral corpus callosum 24 h after permanent MCAO in 4-mo-old mice. Bar, 100 µm. (e and f) Representative image (n = 3) of thionin staining (e) and APC immunostaining (f; green) and DAPI staining (f; blue) in the contralateral and ipsilateral corpus callosum 24 h after permanent MCAO in 9-mo-old mice. Bars: (e) 100 µm; (f) 1 cm. (g) Quantification of OLs (APC^+) in the contralateral and ipsilateral corpus callosum after permanent MCAO in 9-mo-old mice (mean + SEM, n = 3). *, significantly ($P < 0.05$) different from contralateral, Mann-Whitney U test. (h) Representative image (n = 3) of TUNEL staining, APC immunostaining, and active caspase 3 immunostaining in the contralateral and ipsilateral corpus callosum 24 h after permanent MCAO in 9-mo-old mice. Lines show corpus callosum limits. Bars, 100 µm.

animal studies focusing more closely on white matter ischemic lesions are warranted.

In this context, clot lysis by the intravenous injection of recombinant tissue plasminogen activator (tPA; Actilyse) remains the only approved treatment for acute cerebral ischemia. Originally described as a circulating serine-protease, tPA is also expressed within cerebral gray matter by neurons, astrocytes, and microglia (Rogove and Tsirka, 1998; Docagne et al., 1999) and plays various roles primarily related to synaptic formation and plasticity (Frey et al., 1996; Baranes et al., 1998). In pathological conditions, this serine-protease can have detrimental as well as beneficial effects (Benchenane et al., 2004). Through its proteolytic activity, tPA enhances neuronal death by increasing Ca^{2+} entry through the N-methyl-D-aspartate (NMDA) receptor (Nicole et al., 2001) and promoting laminin-dependent anoikis (Chen and Strickland, 1997). In contrast, independently of its protease activity, it can protect neurons from oxidative stress (Kim et al., 1999) and serum deprivation–induced apoptosis (Liot et al., 2006) or it can contribute to microglial activation by binding to annexin II (Siao and Tsirka, 2002).

Earlier studies demonstrated that tPA expression and activity in the cerebral parenchyma decrease during aging, which results in reduced gray matter ischemic lesions (Roussel et al., 2009).

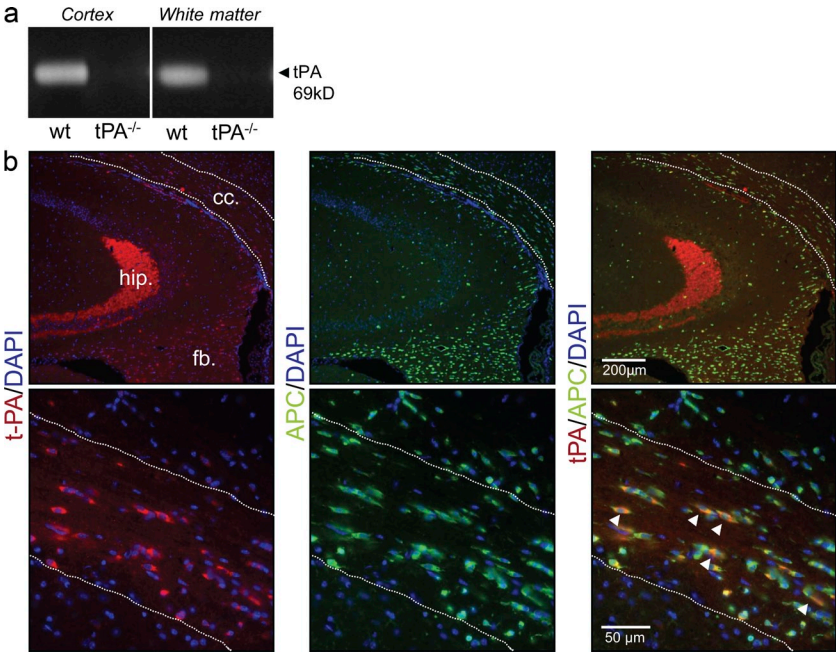

Figure 2. tPA is expressed in OLs of the corpus callosum. (a) Zymography assay shows tPA activity in the cortex and white matter (corpus callosum) of 4-mo-old mice (representative image of $n = 3$). Protein extracts from tPA$^{-/-}$ cortex and corpus callosum appear as a negative control. (b) Photomicrographs of 4-mo-old mice tissue sections show tPA (red, left) or APC (green, middle) immunoreactivities as well as merged image (right). The top (low magnification) shows tPA immunoreactivity is detected in the mossy fiber tract of the hippocampus (hip.), *fimbria* (fb.), and corpus callosum (cc.). The bottom (higher magnification) shows that tPA immunoreactivity is colocalized with APC immunoreactivity in the OLs of the corpus callosum (arrowheads; representative image of $n = 3$).

However, little is known concerning the properties of tPA in cerebral white matter. The first objective of the present study was to determine how aging can influence the extent of white matter ischemic lesions and to understand if tPA can affect these lesions.

Oligodendrocyte (OL) cell death occurs in acute brain diseases such as cerebral ischemia (Pantoni et al., 1996), perinatal hypoxia-ischemia (Ness et al., 2001), or head trauma (Raghupathi, 2004), where it is an important feature of white matter lesions. OL death has been attributed to vulnerability to oxygen free radicals (Husain and Juurlink, 1995), overactivation of glutamate receptors (Sánchez-Gómez et al., 2003), or trophic factor deprivation (TFD; Molina-Holgado et al., 2002), all of which induce apoptosis (Matute et al., 2006; Butts et al., 2008). TFD-induced apoptosis has been used to reproduce features of brain cell injury which can be observed in pathological conditions. For example, loss of trophic signals can occur in the white matter as a consequence of ischemia. In neurodegenerative and demyelinating diseases, injured axons may also be less efficient at producing trophic molecules for cells of the oligodendroglial lineage. In all these cases, apoptosis of OLs may likely result, thus contributing to the white matter lesions. Indeed, Shibata et al. (2000) reported that caspase-mediated apoptosis was responsible for the death of OLs in hypoxic conditions and in cerebral ischemia (Shibata et al., 2000).

The second general objective of the present study was to find out whether tPA could influence OL apoptosis in vitro and white matter ischemic lesions in vivo. We attempted to uncover the molecular mechanisms sustaining this potential effect and, in particular, identify the membrane receptors and signaling pathways involved.

RESULTS

Aging differentially influences gray and white matter susceptibility to stroke

Recent studies suggest that age-related changes in central nervous system tissues could influence white matter injuries (Wasserman and Schlichter, 2008; Baltan, 2009). Although this likely corresponds to an important aspect of human stroke pathology (Baltan, 2009), no study directly addressed this question in animal models of stroke. Our first step was thus to perform permanent middle cerebral artery occlusion (MCAO) in mice at three different ages (4, 9, and 20 mo) and assess the ischemic lesion volume in the gray matter (cortex) and in the white matter (corpus callosum). At 4 mo, MCAO induced extended lesions to the cortical gray matter (Fig. 1, a and c). Nevertheless, barely any lesion was detectable by thionin staining in the white matter of 4-mo-old animals (Fig. 1, b and c), despite a loss of perfusion to the corpus callosum as shown by in vivo lectin-FITC angiography coupled to collagen IV staining (Fig. 1 d). However, although gray matter lesion volume decreased with age (Fig. 1, a and c), as already reported in other models of ischemia (Shapira et al., 2002; Roussel et al., 2009), the damages to white matter after MCAO were increased (Fig. 1, b and c). White matter lesions were more severe in the anterior part of the corpus callosum, remained isolated from gray matter lesions (Fig. 1 e), and were characterized by loss of OLs, as assessed by immunostaining for the OL marker APC (Fig. 1 f) and corresponding quantification (Fig. 1 g). OLs within white matter lesion presented features of apoptotic cell death, such as immunoreactivity for active caspase-3 (Fig. 1 h). TUNEL staining was also detected in the same regions (Fig. 1 h). MCAO also induced a dramatic loss in OL progenitor cells, as assessed by immunostaining for PDGFR-α (Fig. S1 a) and corresponding quantification (Fig. S1 b).

tPA is present in OLs of the corpus callosum and its expression is decreased with age

tPA expression has been largely reported in cells of the gray matter (Rogove and Tsirka, 1998; Docagne et al., 1999).

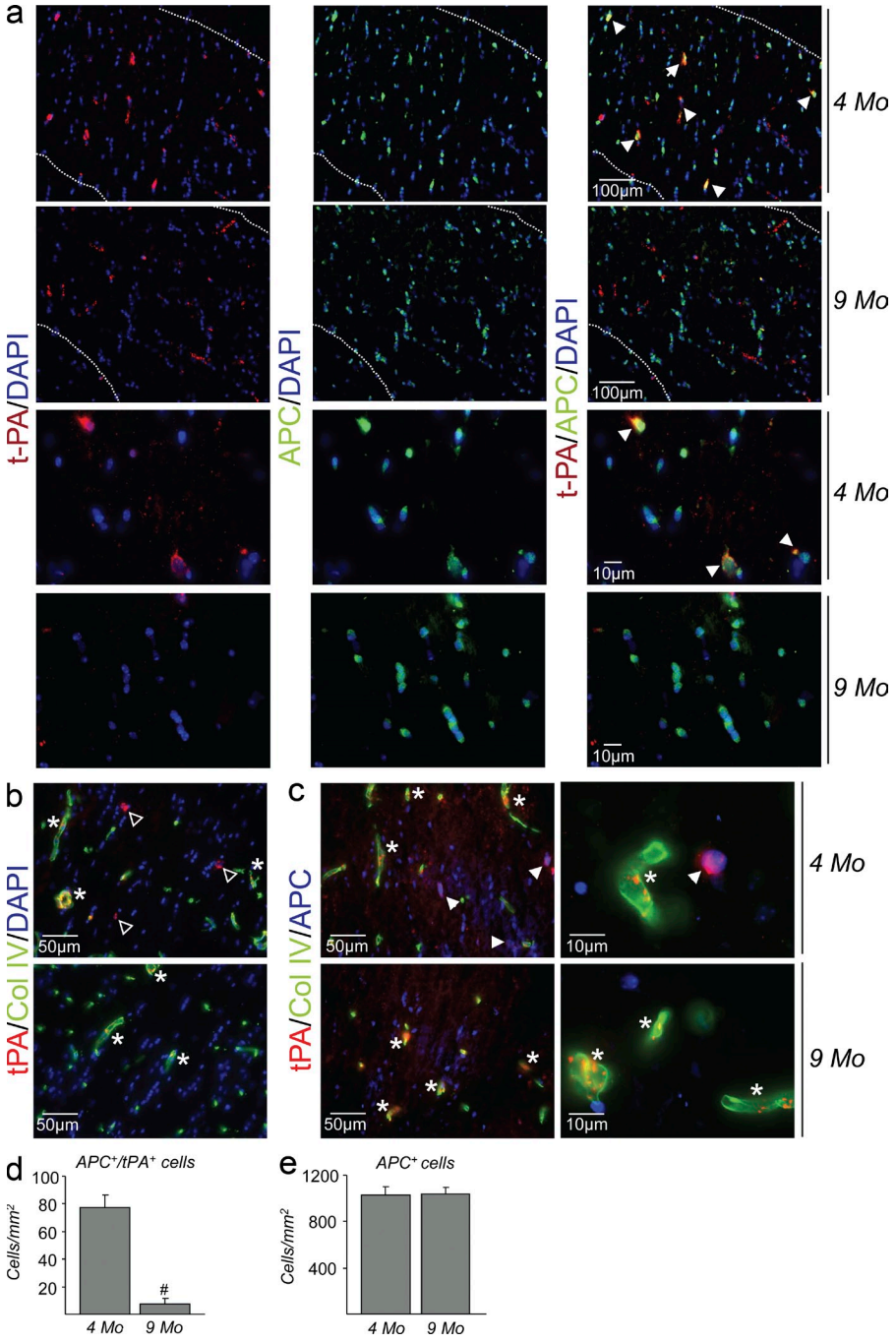

Figure 3. tPA expression in the white matter is altered with age. (a–c) Photomicrographs from 4- and 9-mo-old C57/bl6 mice tissue sections show representative images of tPA (a, b, and c, red), APC (a, green; c, blue), and collagen IV (b and c, green) immunoreactivities in the corpus callosum of young (4 mo) and old (9 mo) mice. Filled arrowheads show colocalization of tPA and APC immunoreactivities. Empty arrowheads show tPA immunostaining not associated with vessels. Asterisks show colocalization of tPA and collagen IV immunostainings. (representative images, $n = 3$). (d and e) Quantification of OLs expressing tPA (APC^+/tPA^+; d) and total number of OLs (APC^+; e) in the corpus callosum of young (4 mo) and old (9 mo) mice (mean + SEM; $n = 3$). #, significantly ($P < 0.05$) different from 4-mo-old mice, Mann-Whitney *U* test.

An earlier study from our group showed that the expression of tPA decreases gradually with age in different areas of the brain (Roussel et al., 2009). However, these changes were not directly addressed in the white matter. In this study, a series of immunostainings was performed to compare the localization of tPA immunoreactivity in the corpus callosum of young (4 mo old) and old (9 mo old) mice. We observed that the colocalization between tPA and APC immunoreactivities was lost in old mice (Fig. 3 a). However, tPA was still detected at this age, although only associated with vessels, as shown by double immunostaining for tPA and collagen IV (Fig. 3 b). A triple immunostaining for tPA, APC, and collagen IV (Fig. 3 c) confirmed these data by showing that in young mice tPA is found in both OLs and vessels, whereas in old mice tPA appears only in vessels.

Nevertheless, its expression in the white matter remains undocumented. In this study, we observed using casein-plasminogen zymography that tPA activity was not only present in the cerebral gray matter (Fig. 2 a, cortex) but also in the white matter (Fig. 2 a, corpus callosum) of young mice (1–2 mo). Coimmunostainings for tPA and APC showed that OLs are the main cell type expressing tPA immunoreactivity in the corpus callosum of these mice (Fig. 2 b). No tPA immunostaining was observed in OL progenitors or microglia of the corpus callosum (Fig. S2, b and c).

tPA protects cultured OLs from apoptotic cell death induced by TFD independently of its interaction with its known partners

Results presented in the previous section show that during aging in mice, tPA immunostaining is lost in OLs of the white matter, whereas this structure shows a greater susceptibility to stroke. This is in opposition to what was reported in the gray matter, where the decrease in tPA expression was associated with smaller ischemic lesions (Wang et al., 1998; Roussel et al., 2009). To explain this difference, we hypothesized that tPA could act on the

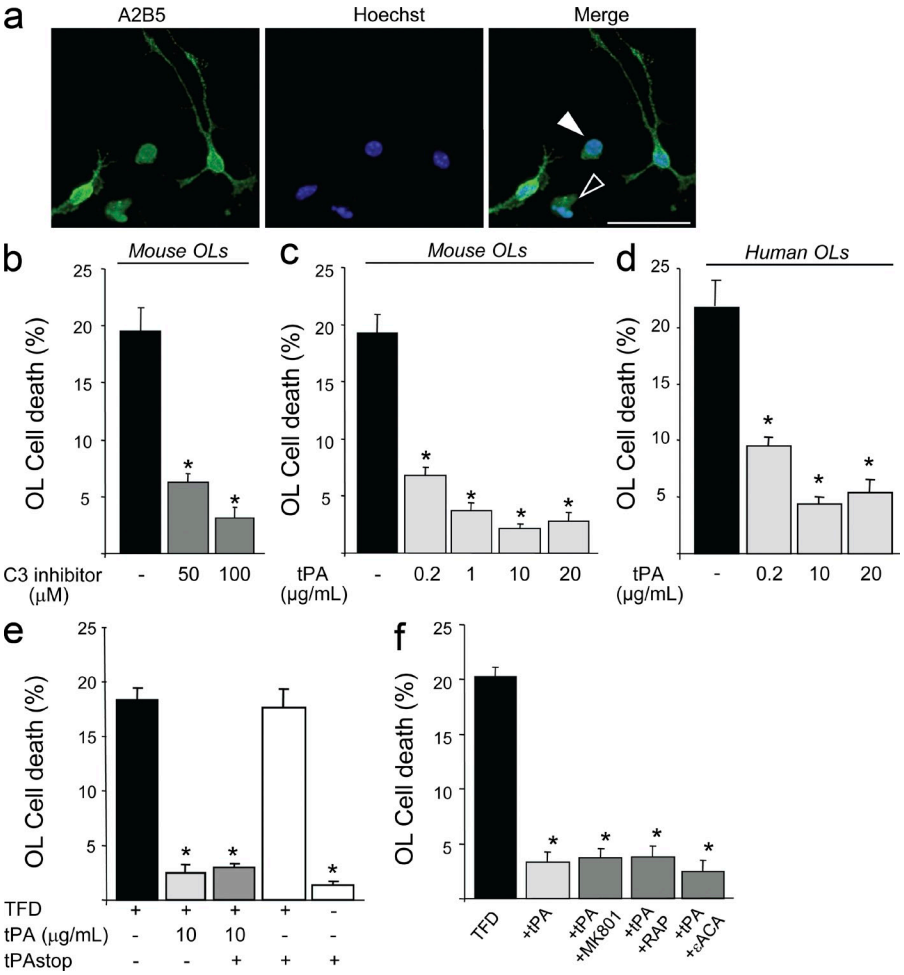

Figure 4. tPA protects mouse and human cultured OLs from apoptotic cell death induced by TFD independently of its classical receptors. (a) Cultured mouse OLs were deprived of trophic factors for 24 h. Photomicrographs show representative fields after A2B5 immunostaining (green) and Hoechst 33258 nuclear costaining (blue). Filled arrowhead, A2B5 cell lacking cell processes; empty arrowhead, A2B5 cell lacking cell processes and chromatin condensation (representative image, $n = 3$). Bar, 100 μm. OL death (percentage) was estimated by measuring the LDH release in the media. (b and c) Mouse OL death was estimated after 24 h of TFD (black bar) and cotreatment with 50 or 100 μM caspase 3 inhibitor (Ac-DEVD-CHO; b, gray bars; mean + SEM; $n = 12$.) or 0.2–20 μg/ml tPA (c, light gray bars; mean + SEM; $n = 12$). (d and e) Human OL death (percentage) was estimated after 72 h of TFD (black bar) and cotreatment with increasing doses of tPA (0.2–20 μg/ml; d, light gray bars; mean + SEM; $n = 12$) in the presence (e, dark gray bar) or absence (e, light gray bar) of 1 μM of the inhibitor of proteolytic activity of tPA, tPAstop (mean + SEM, $n = 12$). (f) Mouse OL death (percentage) was estimated after 24 h of TFD (black bar) and cotreatment with 10 μg/ml tPA in the presence (dark gray bars) or absence (light gray bar) of the following drugs, as indicated: MK801, RAP, and εACA (mean + SEM; $n = 8$, three independent plates). *, significantly ($P < 0.01$) different from TFD.

cells of the gray and white matter in different fashions. We thus investigated whether tPA could influence the survival of OLs.

We used a model of apoptotic death of OLs through TFD. As seen in Fig. 4 a, TFD induced cell body shrinkage and loss of cell processes. Nuclear staining with Hoechst 33258 detected chromatin condensation in OLs (Fig. 4 a). This paradigm induced ∼20% of cell death after 24 h (Fig. 4 b), which is in accordance with previous observations in this (Molina-Holgado et al., 2002) and other (Sánchez-Gómez et al., 2003) models of apoptotic OL death. Cell death was reversed by addition of a caspase 3 inhibitor (Fig. 4 b), confirming that OL death occurred through apoptosis in conditions of TFD. Interestingly, in the presence of 0.2–20 μg/ml of recombinant human tPA (rhtPA), TFD-induced OL death was reduced by ∼70% (Fig. 4 c). The same paradigm was tested on primary cultures of human OLs, which reached 20% of cell death at 72 h (Fig. 4 d). Like in mouse cells, rhtPA induced a protective effect in human OLs (Fig. 4 d).

Next, we attempted to identify the mechanisms underlying the antiapoptotic effects of tPA in OLs. tPAstop is a competitive inhibitor of tPA proteolytic activity that is known to prevent tPA-induced potentiation of excitotoxic neuronal death (Liot et al., 2004). However, tPAstop did not reverse the antiapoptotic effects of rhtPA in OLs (Fig. 4 e). tPA can mediate certain effects through its lysine binding sites (LBSs) or by binding to membrane receptors such as low-density lipoprotein receptor–related protein (LRP; Benchenane et al., 2005) or NMDA receptors (Nicole et al., 2001), or interaction with Annexin II (Lee et al., 2007). rhtPA was incubated with inhibitors of these interactions before testing in the OL apoptotic model. Although NMDA receptors have been identified on OLs (Salter and Fern 2005), MK-801, a potent antagonist of NMDA receptor, did not modify the effects of rhtPA on OL survival (Fig. 4 f). Similarly, incubation of rhtPA with receptor-associated protein (RAP), an antagonist of its interaction with the LRP, had no effect on the rhtPA action in this assay (Fig. 4 f). Last, ε-aminocaproic acid, which is known to antagonize potential interactions with LBS of tPA, also failed to reverse the effects of tPA (Fig. 4 f). These data show that the antiapoptotic effects of tPA on OLs occur regardless of its proteolytic activity or interactions with LBS, and of its known abilities to bind to certain receptors such as NMDA receptors or LRP.

tPA mediates its antiapoptotic effects through an epidermal growth factor (EGF)–like effect

Among other structural motifs, tPA contains a domain of significant homology with the cytokine EGF. We hypothesized that

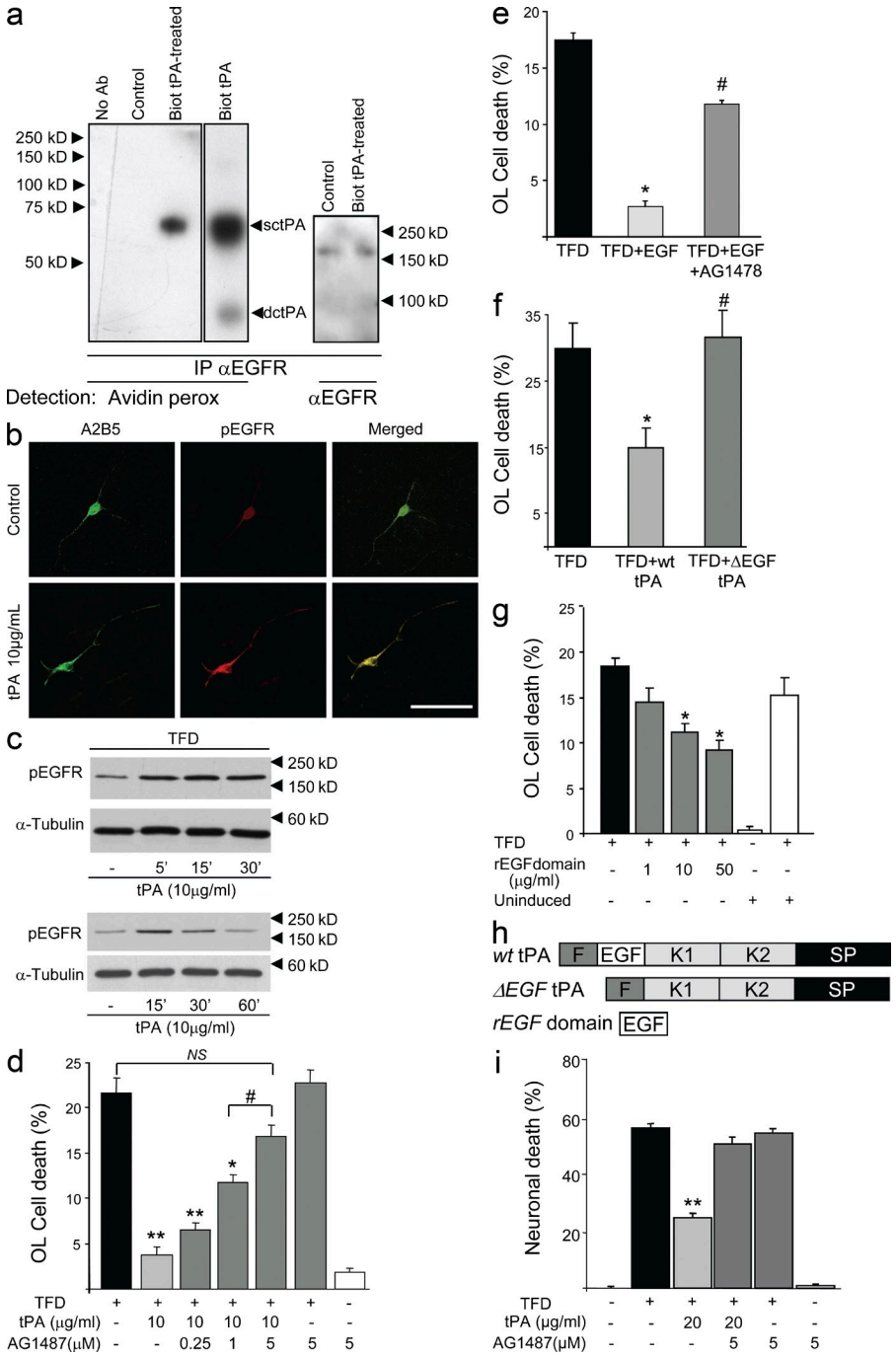

Figure 5. tPA interacts with and activates EGFR to mediate its antiapoptotic effects in OLs. (a) 50 µg of total proteins from lysates of untreated (control) or biotinylated tPA (Biot-tPA)–treated mouse OLs (10 µg/ml) or purified Biot-tPA were subjected to immunoprecipitation using anti-EGFR antibody followed by detection with either peroxidase-coupled avidin (Avidin perox) or with anti-EGFR antisera (αEGFR). As a control, the same procedure was performed by omitting the anti-EGFR antiserum (No Ab). Representative images of immunoblots from three individual experiments are presented. Numbers indicate molecular mass of standard proteins in kilodaltons. Single chain or double chain forms of tPA are indicated as sctPA or dctPA, respectively. (b) Cultured mouse OLs were treated with 10 µg/ml tPA for 24 h or not treated (control). Photomicrographs show representative fields after A2B5 (green) and phosphorylated EGFR (red) immunostaining or the merged images. (c) The phosphorylated form of EGFR was immunodetected in 20 µg of total proteins from OLs subjected to TFD in the presence of 10 µg/ml tPA for the indicated length of time. Anti–α-tubulin was used as a control. Representative images from three individual experiments are presented. Bar, 50 µm. (d–g) Mouse OL death (percentage) was estimated by measuring the LDH release in the media after 24 h of TFD (black bar). (d) Cotreatment with 10 µg/ml tPA (light gray bar) in the presence of 0.25–5 µM AG1487 (dark gray bars; mean + SEM; $n = 12$). * and **, significantly different from TFD, $P < 0.05$ and $P < 0.01$, respectively; #, significantly different from 1 µM AG1487 cotreatment, $P < 0.05$. (e) Cotreatment with 10 ng/ml EGF with or without an inhibitor of the kinase activity of 5 µM EGFR (AG1487; mean + SEM; $n = 8$, three independent plates). #, significantly different from TFD + EGF, $P < 0.05$. (f) Cotreatment with 10 µg/ml of rat recombinant WT or EGF domain–deleted (ΔEGF) tPA (f) or cotreatment with 1–50 µg/ml of a recombinant peptide corresponding to the EGF domain of tPA (rEGF domain) or protein from uninduced bacterial cultures (uninduced) as a control (g; mean + SEM; $n = 8$, three independent plates). *, significantly ($P < 0.05$) different from TFD; #, significantly ($P < 0.05$) different from TFD + *wt*tPA. (h) Diagram of the different mutant forms of tPA used in this study. (i) Mouse neuronal death (percentage) was estimated by measuring the LDH release in the media after 24 h of serum deprivation (black bar) and cotreatment with 20 µg/ml tPA (light gray bar) with or without 5 µM AG1487 (dark gray bars; mean + SEM; $n = 12$). **, significantly different from TFD, $P < 0.01$.

this domain could be responsible for the antiapoptotic effects of tPA. It was thus crucial to determine if tPA could interact with EGF receptor (EGFR). To address this issue, OLs were treated with biotinylated rhtPA, followed by extraction of proteins which were then subjected to immunoprecipitation using an anti-EGFR antibody (Fig. 5 a). Presence of biotinylated rhtPA was detected in the EGFR-immunoprecipitated proteins as an ~70-kD band revealed by peroxidase-coupled avidin (Fig. 5 a) at the same molecular mass as that of biotinylated rhtPA run in parallel (Biot tPA). This protein was absent in untreated cells (control). In parallel, the immunoprecipitated material showed a band at >150 kD corresponding to EGFR, when revealed with anti-EGFR antibodies (Fig. 5 a). These data show that tPA and EGFR are part of a same protein complex in OLs.

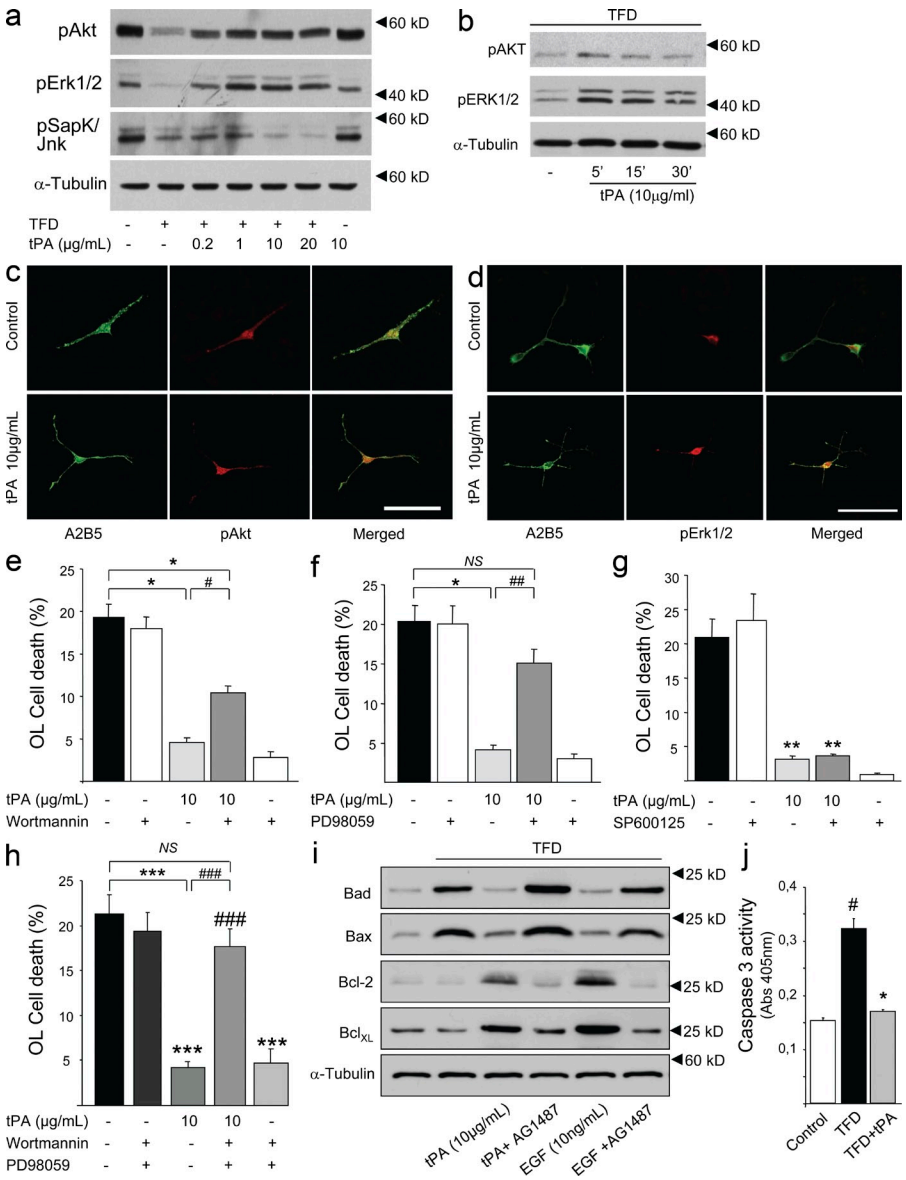

Figure 6. Antiapoptotic effect of tPA is driven by the recruitment of Erk1/2 and Akt intracellular pathways and targets antiapoptotic pathways. (a) Immunodetection of phosphorylated forms (denoted with a prefix, p) of Akt, Erk1/2, or SapK/Jnk in 20 µg of total proteins from lysates of OLs subjected to TFD in the presence of 0.2–20 µg/ml tPA at 24 h. Anti–α-tubulin was used as a control. Representative images of three independent experiments are presented. (b) 20 µg of total proteins from OLs subjected to TFD in the presence of 10 µg/ml tPA at indicated times (minutes) were subjected to immunoblotting and detection of pAkt and pErk1/2. Anti–α-tubulin was used as a control. Representative images from three independent experiments are presented. (c and d) Cultured mouse OLs were treated with 10 µg/ml tPA for 24 h. Photomicrographs show representative fields after A2B5 (green) and phosphorylated Akt (c, red) or phosphorylated Erk1/2 (d, red) immunostaining or the merged images as indicated. Bars, 50 µm. (e–h) Mouse OL death (percentage) was estimated by measuring the LDH release in the media after 24 h of TFD (black bars) or cotreatment with 10 µg/ml tPA (light gray bars) in the presence of inhibitors (dark gray bars) of PI3/Akt (100 nM wortmannin; e) and Erk1/2 (10 µM PD98059; f), SapK/Jnk (10 µM SP600125; g), or both wortmannin and PD98059. (h; mean + SEM; $n = 12$). *, **, and ***, significantly (respectively, $P < 0.05$, $P < 0.01$, and $P < 0.005$) different from TFD; #, ##, and ###, significantly (respectively, $P < 0.05$, $P < 0.01$, and $P < 0.005$) different from TFD + tPA; NS, nonsignificant ($P \geq 0.05$). (i) Immunodetection of Bad, Bax, Bcl-2 or Bcl-XL in 20 µg of total proteins from lysates of OLs subjected to TFD in the presence of 10 µg/ml tPA with or without 5 µM of EGFR kinase inhibitor (AG1487) or 10 ng/ml EGF with or without 5 µM of EGFR kinase inhibitor (AG1487) as indicated. Anti–α-tubulin was used as a control. Representative images from three individual experiments are presented. (j) Caspase-3 cysteine-protease activity (Abs at 405 nm) in extracts (50 µg total proteins /condition) from OLs (control) or OLs subjected to TFD for 24 h, without (black bar) or with (light gray) 10 µg/ml tPA, as determined using a commercial kit. (Mean + SEM, $n = 7$, corresponding to three independent plates). *, significantly ($P < 0.005$) different from TFD; #, significantly ($P < 0.005$) different from control.

We then investigated whether this interaction could induce the activation of EGFR. In the presence of 10 µg/ml rhtPA, EGFR on the OLs appeared to be phosphorylated as detected by immunoblotting and immunohistochemistry using antisera against phospho-tyr1068 of the EGFR (Fig. 5, b and c). Increased phosphorylation of EGFR occurred as early as within 5 min of rhtPA treatment and went back to control levels at 60 min (Fig. 5 c and Fig. S3 show quantification).

Next, we investigated whether the interaction of tPA with EGFR, and the subsequent activation of this receptor, could be responsible for the antiapoptotic effect of tPA on OLs. Interestingly, the inhibitor of EGFR kinase, AG1487, reversed the effect of rhtPA on OLs during TFD in a dose-dependent manner, whereas it showed no effect when applied alone (Fig. 5 d) although tPA mRNA expression and a moderate tPA activity were detected in OLs (Fig. S4). Similarly, 10 ng/ml of recombinant mouse EGF protected OLs against TFD-induced cell death, an effect which was reverted by AG1487 (Fig. 5 e). To further confirm that the EGF-like domain of tPA could be responsible for its antiapoptotic effect in OLs, we constructed two recombinant proteins, one in which the EGF-like domain of tPA (aa 79–117) was deleted (Fig. 5 h, *ΔEGF*tPA) and a second one corresponding to the EGF-like domain of tPA (Fig. 5 h, *rEGF*domain). Interestingly, the antiapoptotic effect of tPA

was abrogated when its EGF domain was deleted (Fig. 5 f, *ΔEGF*tPA). In contrast, 1–50 µg/ml of the rEGF peptide, when applied to OLs in conditions of TFD, induced antiapoptotic effects (Fig. 5 g), albeit with lower efficiency than native tPA. Finally, tPA was also able to induce antiapoptotic effects in neurons (Fig. 5 i), as previously described (Liot et al., 2006), and these effects were also reversed by AG1487 (Fig. 5 i). These data show that the antiapoptotic effects of tPA are mediated by a direct interaction with EGFR and its subsequent activation.

tPA, via extracellular regulated kinase (Erk) 1/2 and Akt intracellular pathways, regulates the balance between pro- and antiapoptotic factors and reduces the activity of caspase 3

EGFR is able to recruit several signaling cascades, including mitogen-activated protein kinase (MAPK)/Erk or phosphoinositide 3 kinase (PI3K)/Akt. In addition, the PI3K–Akt pathway has previously been implicated in OL survival (Vemuri and McMorris, 1996). Moreover, Tyr1068 in EGFR, the residue phosphorylated upon tPA treatment, is involved in the transduction of EGF signal through Erk and Akt pathways (Rojas et al., 1996). Hence, the possible activation of these pathways subsequent to tPA treatment in OLs subjected to TFD was examined. Addition of 0.2–20 µg/ml rhtPA induced the phosphorylation of both Akt and Erk1/2 in a dose-dependent manner, whereas it reduced the phosphorylation of Sap/Jnk, a member of the MAPK family (Fig. 6 a; and Fig. S5, a–c for corresponding quantifications). Activation of Akt and Erk1/2 by tPA treatment occurred within five minutes (Fig. 6 b; and Fig. S5, d and e for corresponding quantifications). Specificity of the cellular location of the phosphorylated forms of Akt and Erk1/2 was confirmed by immunocytochemistry (Fig. 6, c and d).

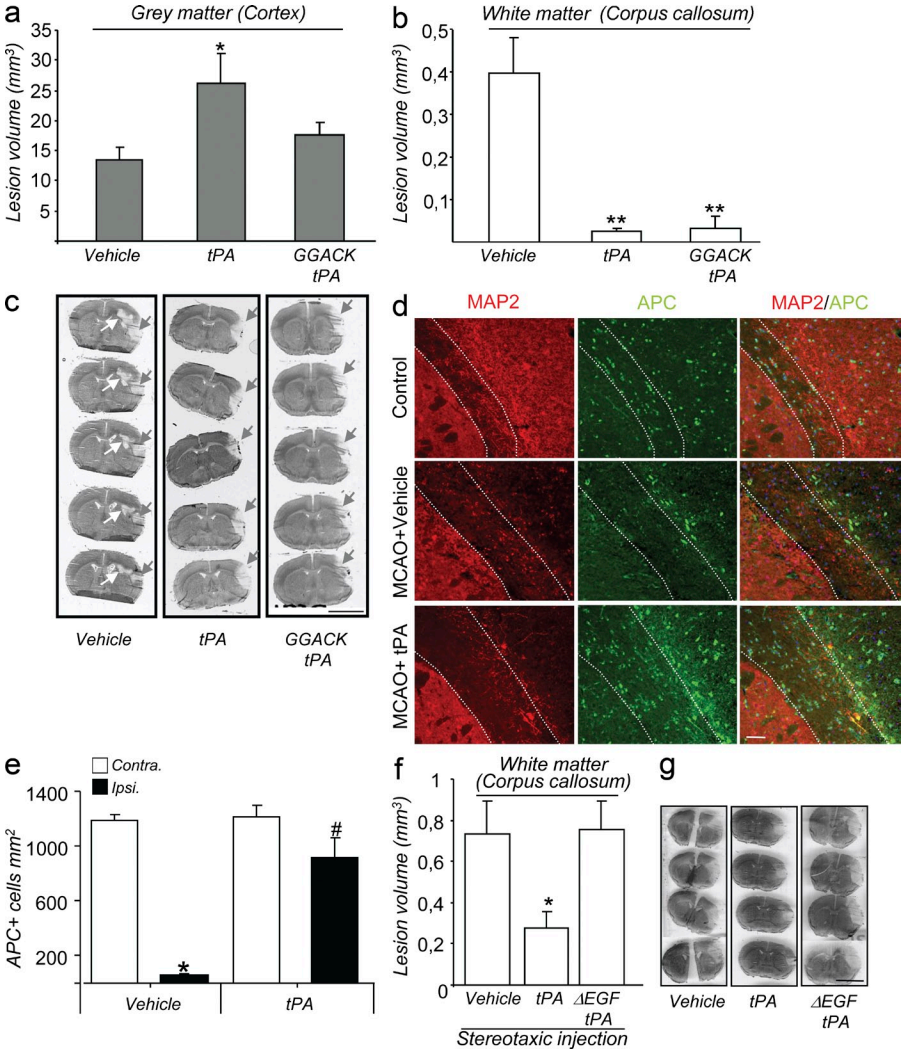

Figure 7. tPA injection reduces ischemic white matter lesions in aged mice independently of its proteolytic activity. (a and b) C57/bl6 mice (9 mo old, five mice per group) were subjected to permanent MCAO 3 h before an intravenous injection of recombinant tPA (Actilyse) in its intact form (tPA) or complexed with the inhibitory peptide, GGACK (GGACK tPA), or corresponding vehicle. Tissue sections were stained with thionin and lesion volumes were estimated in gray matter (cortex; a) and white matter (corpus callosum; b) 24 h after the onset of ischemia (mean + SEM, $n = 5–11$). * and **, significantly (respectively, $P < 0.05$ and $P < 0.01$) different from vehicle, Mann-Whitney *U* test. (c) Representative thionin-stained tissue sections from mice subjected to MCAO. White arrows show white matter lesions, and gray arrows show gray matter lesions. Bar, 1 cm. (d) Photomicrographs of tissue sections from 9-mo-old mice show MAP-2 (red) or APC (green) immunoreactivities, as well as merged images in corpus callosum in the indicated conditions. Control animals, MCAO (ipsilateral hemisphere) with or without i.v. injection of recombinant tPA (Actilyse). Demarcations show the limits of corpus callosum. Bar, 100 µm. Note the loss of both MAP-2 and APC staining after MCAO in vehicle-injected animals. In tPA-injected MCAO animals, only MAP-2 staining is lost, whereas APC staining is preserved. (e) Quantification of OLs (APC^+) in the contralateral and ipsilateral corpus callosum after permanent MCAO in 9-mo-old, vehicle, or tPA-injected animals. *, significantly ($P < 0.05$) different from contralateral; #, significantly ($P < 0.05$) different from vehicle, ipsilateral Mann-Whitney *U* test. (f) C57/bl6 mice (9 mo old, five mice per group) were subjected to permanent MCAO 15 min before an intracerebral injection of recombinant rat tPA, recombinant ΔEGFtPA, or corresponding vehicle. Tissue sections were stained with thionin and lesion volumes were estimated in white matter (corpus callosum) 24 h after the onset of ischemia (mean + SEM; $n = 4–6$). *, significantly ($P < 0.05$) different from vehicle, Mann-Whitney *U* test. (g) Representative thionin-stained tissue sections from mice subjected to MCAO and indicated stereotaxic injections. Bar, 1 cm.

Moreover, pretreatment with an inhibitor of the activation of PI3K–Akt pathway (wortmannin; Fig. 6 e) or with an inhibitor of MEK–Erk1/2 pathway (Fig. 6 f, PD98059) both partially reversed the protective effect of rhtPA on OLs during TFD. In contrast, no effect was observed when inhibiting the phosphorylation of SapK/Jnk with SP600125 (Fig. 6 g). However, cotreatment with both wortmannin and PD98059 completely reversed the protective effect of rhtPA on OLs during TFD (Fig. 6 h). Together, these data show that the antiapoptotic effect of tPA is driven by the recruitment of Erk1/2 and Akt intracellular pathways.

Apoptosis is regulated by a balance between pro- and antiapoptotic factors that control downstream protease activity of effector caspase, caspase 3, and subsequent cell death. In this paper, we studied the expression of two proapoptotic factors (Bad and Bax) and two antiapoptotic factors (Bcl-2 and Bcl-$_{XL}$) in OLs submitted to TFD, and their possible regulation by tPA. We observed that TFD induced the up-regulation of Bad and Bax without affecting the expression of Bcl-2 or Bcl-$_{XL}$ (Fig. 6 i; and Fig. S5, f–i for corresponding quantification), leading to an increase in the ratio between pro- and antiapoptotic factors. Treatment with 10 µg/ml rhtPA brought Bad and Bax expression back to basal levels, whereas it induced the up-regulation of Bcl-2 and Bcl-$_{XL}$ (Fig. 6 i; and Fig. S5, f–i for corresponding quantification), thus reducing the ratio between pro- and antiapoptotic factors. The cotreatment with AG1487 completely reversed these effects of rhtPA (Fig. 6 i; and Fig. S5, f–i for corresponding quantification). Moreover, EGF induced effects similar to those observed with rhtPA (Fig. 6 i; and Fig. S5, f–i for corresponding quantification). Finally, although TFD led to an increase in caspase 3 activity, no difference in this activity could be observed between control and rhtPA-treated cells (Fig. 6 j). These data show that EGF-like activity of tPA targets antiapoptotic pathways in OLs subjected to TFD.

tPA reduces ischemic white matter lesions in aged mice through its EGF domain, independently of its proteolytic activity

The results in the previous section show that tPA displays antiapoptotic properties in OLs (Figs. 4–6). We therefore hypothesized that in old animals, where white matter lesions are associated with OL cell death (Fig. 1), the application of recombinant tPA could limit OL cell death and, thus, result in white matter protection.

To verify this hypothesis, we subjected 9-mo-old mice to MCAO and injected them intravenously with recombinant rhtPA (Fig. 7). This injection was performed at 3 h after the onset of ischemia, which fits with the window of therapeutic opportunity approved for rhtPA treatment in humans (Lansberg et al., 2009). MCAO in these animals induced both gray matter and white matter lesions (Fig. 7). The injection of rhtPA resulted in a potentiation of gray matter lesions (Fig. 7, a and c), as previously observed (Wang et al., 1998; Nagai et al., 1999; Kilic et al., 2001). In accordance with previous studies, this potentiation was a result of the proteolytic activity of tPA (Nicole et al., 2001), as this effect was no longer observed when the enzymatic activity of tPA was blocked by the inhibitory peptide GGACK (Fig. 7, a and c). In sharp contrast, white matter lesions (Fig. 7, b and c) and loss of APC$^+$ cells (Fig. 7, d and e) were reduced by the injection of rhtPA, results which emphasize the protective effects of tPA on white matter tissues. No effect of tPA administration was observed on microglial response within the injured white matter (Fig. S6, a–c). Myelin integrity was also conserved after tPA injection in MCAO and control animals (Fig. S6 d). Strikingly, and in accordance with what we described in this paper in the in vitro model of OL cell death, tPA exerted this action independently of its protease activity, as GGACK-tPA was as effective as the proteolytically active rhtPA in reducing white matter lesions (Fig. 7, b and c). When injected directly into the corpus callosum, tPA also reduced white matter lesions induced by MCAO (Fig. 7, f and g). Noticeably, the deletion of EGF domain invalidated this protective action, as the stereotaxic injection of ΔEGFtPA did not modify white matter lesion volume after MCAO (Fig. 7 f).

Finally, MCAO was induced in tPA$^{-/-}$ mice (Carmeliet et al., 1994) and lesion volumes were compared with WT animals. Lesion volume was reduced in the gray matter of tPA$^{-/-}$ animals (not depicted), as previously reported (Nagai et al., 1999; Roussel et al., 2009). However, white matter lesion volume was unchanged in tPA$^{-/-}$ as compared with WT animals (unpublished data).

DISCUSSION

We report in this paper that cytokine effects of tPA protect white matter from age-dependent stroke lesions based on the following observations: (1) tPA expression is decreased along aging in the white matter; (2) this decrease accompanies the emergence of a vulnerability of white matter to ischemia; (3) tPA plays an antiapoptotic role in OLs, the survival of which is critical for white matter integrity; (4) this antiapoptotic action is mediated through an EGF-like effect; and (5) when injected into aged animals, tPA drastically reduces ischemic lesions to the white matter. This study emphasizes aging as a critical factor for stroke-induced white matter lesions. Indeed, young animals (4 mo) hardly show any white matter lesion after permanent MCAO. But in older animals (>9 mo), lesions to the white matter become evident. Considering these results, the use of young animals in most experimental studies may have put a strong brake on research on white matter lesions in cerebral ischemia. The use of aged animals could then represent a relevant approach and a good alternative to the models of white matter lesions, such as stereotaxic injection of vasoconstrictor molecules (Sozmen et al., 2009) or ex vivo models of oxygen and glucose deprivation (Baltan, 2009). This is of special interest when one considers the fact that aging is one of the crucial risk factors for stroke in humans.

What can then be the factors that render white matter susceptible to ischemia when animals grow old? Several facts pointed out tPA as a candidate of choice. Interestingly, the expression of tPA appears to be regulated by age in the central

nervous system, where it can influence severity of ischemia in an age-dependent manner (Roussel et al., 2009). Moreover, although white matter lesions were not addressed in this previous study, tPA has been reported to influence white matter physiopathology in experimental models of nerve injury (Minor et al., 2009), preterm excitotoxic lesions (Hennebert et al., 2004), or multiple sclerosis (Lu et al., 2002), for instance. However, how tPA can influence the outcome of white matter tissues after stroke was unknown, and study of these effects appears to be mandatory when one considers that tPA is the only approved treatment for acute stroke in humans.

The present study is the first to address the effect of tPA on apoptosis in OLs, and it concludes that tPA has antiapoptotic properties on these cells. This contrasts with earlier studies in neurons, in which tPA exacerbates excitotoxic death and displays proapoptotic (Flavin et al., 2000; Liu et al., 2004) and antiapoptotic (Liot et al., 2006; Lee et al., 2007) effects. These opposite effects may explain why, when injected into mice subjected to MCAO, tPA aggravates gray matter lesions, whereas it reduces white matter lesions (Fig. 7).

Although most of the functions of tPA are driven by its serine-protease activity, growing evidence indicates that nonproteolytic activities are also important (Yepes et al., 2009). The present study shows for the first time that independently of its proteolytic activity, but by binding to and subsequently inducing phosphorylation of EGFR, tPA can induce antiapoptotic effects in OLs. Overall, our study suggests that by the virtue of its EGF-like domain, tPA could substitute the classical trophic molecules, such as cytokines or growth factors, and promote survival of OLs. Consequently, the prosurvival action of tPA would be redundant of other cytokines, which suggests that tPA can, in certain conditions, be regarded as a component of the cytokine network.

Two earlier studies linked tPA to EGF signaling (Hurtado et al., 2007; Ortiz-Zapater et al., 2007), although in a different process (proliferation), in a different cell type (pancreatic cells), and by the following different mechanisms: (1) tPA, via the sequential action of plasmin and metalloproteinase 9 can activate heparin-bound EGF into free EGF, leading to subsequent EGF signaling (Hurtado et al., 2007); and (2) tPA can induce its action through binding to EGFR (Ortiz-Zapater et al., 2007) but, in contrast to our results, dependently of Annexin A2. These different data underline the variety that exists in the mechanisms of action of tPA, depending on the biological context in which this molecule is found.

Several paradigms of OL cell death have been used in vitro, such as nitric oxide toxicity (Baud et al., 2004), hyperoxia (Gerstner et al., 2006), excitotoxicity (Sánchez-Gómez et al., 2003), or growth factor deprivation (Molina-Holgado et al., 2002), all of which induce apoptosis. Remarkably, despite the variety in the nature of compounds displaying antiapoptotic properties in these models, one common factor in their mechanisms of action is the activation of the PI3K–Akt pathway, as also observed in the present study (Fig. 6).

In this study, we show that in conditions of TFD, tPA reduces the levels of the proapoptotic factors Bad and Bax and increases the antiapoptotic factors Bcl-2 and Bcl-$_{XL}$. These changes finally lead to a modification of the ratio between pro- and antiapoptotic factors in favor of antiapoptotic factors. These effects were mediated through EGFR activation and subsequent recruitment of PI3K–Akt and Erk1/2 pathways. Accordingly, EGF has been shown to induce antiapoptotic effects in various cell types through PI3K–Akt and Erk1/2 pathways, which can inhibit proapoptotic factors or activate antiapoptotic factors (Henson and Gibson, 2006).

The lack of difference in white matter lesion volume between WT and tPA$^{-/-}$ animals contrasts with the extensive literature reporting phenotypes in the brain of tPA$^{-/-}$ mice. However, cytokine effects of tPA were usually not addressed in these previous studies. For instance, reduction of gray matter lesions in tPA$^{-/-}$ mice, reported previously (Nagai et al., 1999; Roussel et al., 2009), is generally attributed to proteolytic effects of tPA. This is in agreement with one of the general conclusions of this study, which is that tPA differently affects the susceptibility of white and gray matter to stroke-induced lesions. These differential effects account for distinct mechanisms of action of tPA (proteolytic vs. nonproteolytic) depending on the brain structure. Several hypotheses could explain the lack of phenotype in the ischemic white matter of tPA$^{-/-}$ animals, such as putative compensatory mechanisms or redundancy of tPA cytokine effects to other cytokines. Future studies using pharmacological inhibitors or siRNA might be helpful to discern potential compensatory effects in the white matter and allow one to discern the necessity and sufficiency of tPA for protection. Overall, these different points raise the question of the respective effects of endogenously produced versus exogenously delivered tPA. Although our study focused on the potential therapeutic effects of exogenously applied tPA, further investigations should be initiated to better understand the role of endogenous tPA in white matter stroke lesions.

One essential observation was that although tPA reduces white matter lesions after cerebral ischemia, it exacerbates gray matter lesions, as was previously observed in other models of stroke (Benchenane et al., 2004). The latter effect has been attributed to a proteolytic action leading to the potentiation of NMDA-mediated excitotoxic lesions (Nicole et al., 2001). Accordingly, in the present study, when the protease activity of tPA was blocked (GGACK-tPA), its injection no longer affected gray matter lesion volume. Interestingly, protease-inactivated tPA nevertheless remained as efficient as native tPA in reducing white matter damage. This is in agreement with our description of a protease-independent protective effect of tPA on OLs.

To summarize these data, tPA would act as a double-edged sword when it enters the brain parenchyma: on the one hand, it induces a deleterious effect in the gray matter as a result of the cleavage of the NMDA receptor and subsequent potentiation of excitotoxicity in neurons; on the other hand, it provides a beneficial effect in the white matter as a result of the activation of EGFR and subsequent protection against apoptosis in OLs. The present work fits with the idea that the

different domains of tPA can play distinct and even opposite roles in the physiopathology of the brain. Hence, understanding their respective functions is crucial to adapt the use of plasminogen activators in acute stroke management and to design new and more efficient molecules.

MATERIALS AND METHODS

Materials. AG1478 was obtained from Tocris Bioscience. Caspase 3 inhibitor was obtained from Enzo Life Sciences. rmEGF, MK801, ε-aminocaproic acid, tPAstop, and the mouse anti–mouse α-tubulin antibody were obtained from Sigma-Aldrich. Rabbit anti–mouse pErk1/2 and pAkt and anti–mouse phosphorylated EGFR antibodies were obtained from Cell Signaling Technology. Caspase 3 activity detection kit was obtained from Invitrogen. Anti–rabbit IgG antibody was obtained from Jackson ImmunoResearch Laboratories, Inc. and anti–mouse IgG antibody was obtained from Bio-Rad Laboratories. Human rt-PA (Actilyse) was obtained from Boehringer Ingelheim and was dialyzed using membranes that exclude molecules with a molecular mass <10 kD. This procedure allows, in particular, the removal of arginine and small peptides contained in the solution. Monoclonal anti–mouse A2B5 antibody was a gift from M. Holgado (National Hospital for Paraplegics, Toledo, Spain). RAP was provided by G. Bu (St. Louis Children's Hospital, St. Louis, MO).

Animals and surgery. C57BL6-J mice (aged 4, 9, and 20 mo; Janvier) were housed in a temperature-controlled room on a 12-h-light/12-h-dark cycle with food and water ad libitum. Experimental protocols were approved by the regional committee of ethics of Lower Normandy (accredited establishment number C14118001). Experiments were performed in accordance with French ethical laws (act no. 87–848; Ministère de l'Agriculture et de la Forêt) and the European Communities Council Directives of November 24, 1986 (86/609/EEC) guidelines for the care and use of laboratory animals. The middle cerebral artery (MCA) was permanently occluded (MCAO) by electrocoagulation under anesthesia with isoflurane (induction 5%, maintenance 2.5% in 70/30% NO_2/O_2). Rectal temperature was maintained at 37°C using a feedback-regulated heating pad. Mice were placed in a stereotaxic frame, the skin between the right ear and the right eye was incised, and the temporal muscle was carefully retracted. The MCA was exposed and permanently occluded by electrocoagulation. After this surgical procedure the skin was glued with cyanoacrylate and animals were allowed to recover. For in vivo tPA studies, mice were anesthetized with 3 ml after MCAO and injected with a bolus of 10 mg/kg tPA, 10 mg/kg GGACK-tPA, or an equivalent volume of saline through a catheter inserted into the tail vein.

For stereotaxic injections, a microinjection pipette (internal diameter 0.32 mm and calibrated at 15 mm/µl; Hecht Assistent) was stereotaxically implanted in the right corpus callosum (anteroposterior, −0.2; lateral, −3; dorsoventral, −1.9) in anesthetized mice and left for 10 min before 2 µg tPA or its EGF-lacking mutein were injected in a total volume of 2 µl. The pipette was removed 5 min later. Thereafter, mice underwent permanent MCAO as described in the previous paragraph. Time between tPA injection and artery occlusion ranged between 15 and 18 min.

24 h after ischemia, mice were euthanized. The brains were removed and frozen in isopentane for histological analysis. Cryostat-cut coronal brain sections (20 µm) were stained with thionine. For volume analysis, 1 section out of every 10 was stained and analyzed using ImageJ (National Institutes of Health). The lesion volume was estimated as the sum of every lesion area (unstained region) for each section, multiplied by the distance between each section (0.2 mm).

Immunohistochemistry. Mice were deeply anesthetized and perfused transcardially with 20 ml of cold heparinized NaCl 0.9%, followed by 2% paraformaldehyde and 0.2% picric acid in 150 ml of 0.1 M sodium phosphate buffer, pH 7.4. Brains were removed, washed in veronal buffer containing 20% sucrose, and frozen in Tissue-Tek (Miles Scientific). 10-µm coronal sections were incubated overnight at room temperature with a primary antibody directed against tPA (rabbit anti-tPA, 1:1,500; gift from H.R. Lijnen, Center for Molecular and Vascular Biology, University of Leuven, Leuven, Belgium; Declerck et al., 1995; Roussel et al., 2009; Baron et al., 2010), APC (Mouse monoclonal anti-APC, 1/600; ab16794; Abcam), type IV collagen (goat anti–collagen IV, 1:1,500; SouthernBiotech), PDFGR-α (rat anti-CD140a, 1:800; BD), or different combinations of these antibodies. Potential unspecific staining with tPA antibody was blocked by pretreating this antibody with $tPA^{-/-}$ protein extracts. The following protocol was used to perform this blockade: brains from $tPA^{-/-}$ animals were isolated and frozen. A tissue suspension was then obtained by dissociation in saline before incubation at 4°C for 5 min. After treatment with acetone (4:1) and vigorous shaking, the precipitate was recovered by centrifugation at 10,000 *g* for 10 min. The precipitate was finally dried at room temperature until obtaining a powder. This powder was added to the antibody at a concentration of 1%. By using this technique, signal given by this antibody was completely shut down in $tPA^{-/-}$ animals (Fig. S2 a). All our tPA immunostainings were performed using this treated tPA antibody. Detection was performed using donkey TRITC- or FITC-conjugated secondary antibodies (1:500; Jackson ImmunoResearch Laboratories, Inc.). Sections were examined with a microscope (DM6000; Leica). Images were digitally captured using a camera (CoolSNAP; Photometrics) and visualized with MetaVue software (Molecular Devices). For each set of immunostaining, the following controls were systematically performed in adjacent sections: (1) Single immunolabeling, with omission of primary antibodies: no signal detected (excludes unspecific signal given by the secondary antibody); (2) single immunolabeling with omission of secondary antibodies: no signal detected (excludes signal given by autofluorescence of the tissues); (3) coimmunostaining (tPA and cell markers) revealed by another set of secondary antibodies, colocalization of both immunostaining (same pattern of expression); (4) absence of cross-reactivity between the antibodies in multi-immunolabeling experiments demonstrated by a set of stainings in which each of the primary antibodies was, respectively, omitted; (5) absence of irrelevant signal detection when using only the cocktail of secondary antibodies.

In vivo lectin-FITC angiography. In vivo lectin-FITC angiography was performed as previously described (Thiyagarajan et al., 2008). In brief, FITC-labeled *Triticum vulgaris* lectin (Sigma-Aldrich) at 10 mg/kg was administered via the tail vein in anesthetized mice 3 h after MCAO. Mice were euthanatized 2 min after lectin administration and transcardiac perfusion of ice-cold heparinized saline was performed followed by fixation with picric acid and paraformaldehyde. Brains were removed and processed for immunohistological analysis as described.

TUNEL staining. TUNEL staining was performed from 10-µm frozen tissue sections using the in situ cell death detection kit fluorescein (Roche) according to the manufacturer's instruction.

Image analysis and quantification. The image analysis was performed using ImageJ software. The total number of OLs (APC-positive cells) and tPA expressing OLs (APC-positive/tPA-positive cells) was determined in the anterior part of the corpus callosum of healthy mice or mice subjected to MCAO (4 or 9 mo) immunostained for tPA and APC. All quantitative analysis was done in three randomly selected sections per mouse (three mice per condition).

Casein-plasminogen zymography assay. In brief, 5 µg of protein extracts were resolved on SDS–PAGE (12%) containing 1 mg/ml casein and plasminogen. After migration, the gel was washed in 2.5% Triton X-100 solution and incubated for 2 h in a buffer containing 100 mM glycine and 10 mM EDTA, pH 8.3. Light bands indicating proteolytic activity were visualized by Coomassie staining.

OL cell cultures. OL cell cultures were prepared as previously described (Molina-Holgado et al., 2002) from postnatal day 0 (P_0)–P_1 newborn mice from P_0-P_1 newborn mice. After 10 d in vitro, a confluent culture was obtained, composed of microglia and OLs on top of a confluent monolayer of astrocytes. Cells were shaken at 225 rpm at 37°C for 3 h to remove microglia.

A second cycle of shaking was then performed (285 rpm, 37°C, overnight) to remove OLs from the astrocytes monolayer. The cell suspension was plated on bacterial grade Petri dish for 2 h to separate OLs from remaining microglia. Purified OLs (1.25×10^5 cells/cm^2) were cultured in DME/F12 (1:1) supplemented with 5 ng/ml each of recombinant PDGF-AA and bFGF and B27. Experiments were performed at 1 d in vitro. TFD was performed by switching cells to DME/F12 medium lacking PDGF-AA, bFGF, and B27.

Human cultures. Human cultures were established from brain tissues of aborted human brain fetuses after 10–12 wk of gestation. The protocol for tissues so obtained complied with institutional and national guidelines. OL cultures were obtained according to the same method as the one used for mouse cell cultures.

Neuronal cultures. Neuronal cultures were prepared as previously described in Liot et al. (2006). Apoptosis was induced in these cells at 7 d in vitro by switching cells to DME medium lacking serum.

Immunocytochemistry in cultured cells. Immunocytochemistry in cultured cells was performed as described previously (Molina-Holgado et al., 2002). In brief, cells plated onto PDL-coated coverslips were incubated for 1 h at room temperature in PBS containing 5% fetal goat serum with primary antibodies for A2B5 (1:50). After being rinsed with PBS, the cells were incubated for 1 h at room temperature with secondary Alexa Fluor–conjugated anti–mouse IgG. Then the coverslips were washed with PBS and mounted on slides. Nuclei were co-labeled with 1 µg/ml Hoechst 332583 for 10 min at room temperature. Absence of nonspecific interactions was verified by omitting the primary antibodies.

Immunoprecipitation. Specific antisera were added to cell lysates and allowed to react for 2 h at 4°C before adsorption to protein G–Sepharose (GE Healthcare). The resin was washed three times and bound proteins were eluted in a buffer containing DTT and β-mercaptoethanol.

Immunoblotting. Cell lysates were mixed with 5× Laemmli sample buffer and held at 95°C for 5 min. 20 µg of proteins/condition was resolved on 10% SDS-PAGE and electroblotted onto nitrocellulose membrane. Membranes were blocked for 1 h at room temperature in 5% (wt/vol) dry skim milk in TBS with 0.1% Tween 20 (TBST), incubated overnight at 4°C with the corresponding primary antibodies as previously described (Correa et al., 2005), and extensively washed with 5% milk-TBST solution before incubation with secondary antibodies for 1 h at room temperature. Finally, the blots were rinsed and the peroxidase reaction was developed by enhanced chemiluminescence (GE Healthcare). The blots were stripped in 62.5 mM Tris-HCl, pH 6.8, containing 2% SDS and 0.7% β-mercaptoethanol and were reprobed sequentially.

Quantification of cell death. OL cell death was estimated by A2B5 immunostaining and examination of the cultures under bright-field microscopy, and quantified by measurement of lactate dehydrogenase (LDH) release from damaged cells into the bathing medium. The LDH level corresponding to complete cell death was determined in sister cultures exposed to 1% Triton X-100 for 24 h (full kill, FK). Background LDH levels were determined in sister cultures subjected to sham wash (blank, BK). Percentage of cell death in experimental conditions was calculated using the following formula: [% of cell death = (experimental value − BK) × 100/(FK − BK)].

Caspase activity assay. Colorimetric detection of caspase 3 cysteine-protease activity in extracts of OL cultures (50 µg of total proteins/condition) was performed through the use of the Apotarget commercial kit (Invitrogen).

Construction and production of recombinant proteins. For the His-tagged EGF-like tPA-derived domain, the region of *Rattus norvegicus* tPA cDNA (Uniprot ref P19637) encoding aa 79–117 (EGF-like domain) was amplified using the upstream primer 5′-CCGGGATCCCCCGTCCGAAGTTGC-3′ and downstream primer 5′-GGCAAGCTTATCACAGCGTTTCCCAAC-3′, thus introducing a BamHI and a HindIII restriction site (underlined), respectively, for insertion in pQE100-Double Tag vector (QIAGEN), which provides 6xHis at the amino terminus of the insert. The cloned insert was sequence-verified. Recombinant peptide was purified in buffer containing 8M urea, from inclusion bodies of isopropyl 1-thio-β-D-galactopyranoside (IPTG)–induced bacterial cultures (*Escherichia coli*, M15 strain), on a nickel affinity matrix as described by the manufacturer (QIAGEN). Desalting of the relevant fractions was performed using PD MidiTrap G-10 (GE Healthcare) to remove urea. The recombinant peptide corresponding to the EGF-like domain, thus obtained, was equilibrated and allowed to refold in PBS containing Tween 80 (0.5%).

For WT tPA and ΔEGFtPA, rat tPA sequence signal (aa 1–32) was amplified from the full-length *Rattus norvegicus* tPA cDNA (Swiss-prot accession P19637) using the upstream primer 5′-CGGCTAGCATGAAGGGAGAGCTGTTG-3′ and the downstream primer 5′-GCGGATCCGTGATGGTGATGGTGATGCCGAGCTCCTCTTCT-3′, thus including the NheI and BamHI restriction sites (underlined), respectively, and a 6xHis tag just before the BamHI site. PCR products were digested and inserted into the eukaryotic expression system pcDNA5/FRT. Coding sequence for mature rat WT tPA WT and ΔEGFtPA proteins were amplified from the same tPA cDNA sequence by using the appropriate primers. Deletion of the EGF domain was obtained by fusing the PCR product corresponding to the finger and K1 domains of tPA with the PCR product corresponding to the protease domain of tPA. PCR products were inserted into pcDNA5/FRT plasmid between the BamHI and XhoI restriction sites. The various plasmids obtained were systematically checked by automated sequencing (GATC-Biotech). 293 HEK FlpIn Cells (Invitrogen) were then transfected using Lipofectamine 2000 and positive clones were isolated using a 300-µg/ml hygromycin B (Sigma-Aldrich) selection. Supernatants containing tPA-related muteins were harvested and the proteins of interest purified on a nickel affinity matrix (QIAGEN) as described by the manufacturer. Elimination of imidazole was performed by overnight dialysis against 0.5 M ammonium bicarbonate buffer. After concentration using Amicon Ultra (cutoff, 10 kD; Millipore), recombinant proteins were subjected to zymography to assess their enzymatic activity and confirm their molecular mass.

Production of proteolytically inactive tPA (GGACK tPA). A fourfold molar excess of GGACK (1,5-dansyl-L-glutamyl-L-glycyl-L-arginine chloromethylketone; EMD) was added to Actilyse (Boehringer Ingelheim) and allowed to react for 24 h at room temperature. The resulting solution was dialyzed for 48 h at 4°C against PBS to remove all unbound GGACK. Arginine monohydrochloride (Sigma-Aldrich) was added to GGACK-tPA to reconstitute Actilyse buffer. A spectrozyme assay (American Diagnostica) was performed to confirm the lack of proteolytic activity of GGACK-tPA.

Statistical analysis. All results are expressed as mean + SEM. For in vitro experiments, the *n* value corresponds to *n* different well pools derived from three independent dissections. Statistical analyses consisted of one-way ANOVA, followed by Bonferroni–Dunn's test. Results of animal experiments were analyzed by Mann-Whitney's *U* test.

Online supplemental material. Fig. S1 shows loss of OL progenitor cells in the white matter after MCAO. Fig. S2 shows that tPA immunostaining is absent in microglia and OL progenitor cells of white matter. Fig. S3 shows quantification of Western blots showing the phosphorylation of EGFR after tPA treatment. Fig. S4 shows tPA expression in cultured OLs. Fig. S5 shows quantification of Western blots for intracellular pathways and pro/antiapoptotic factors. Fig. S6 shows that tPA does not influence microglial response or myelin integrity in the white matter after MCAO. Online supplemental material is available at http://www.jem.org/cgi/content/full/jem.20102555/DC1.

We are grateful to Anuradha Alahari for critical reading and editing of the manuscript. We would like to thank Laurent Plawinski, Joaquín Sancho, and Elisa Baides for their excellent technical assistance.

This work was performed within the framework of the Plan de Acciones Integradas (PAI-PICASSO) between Spain and France (HF2004-236). It was supported by grants from the Spanish MCI (Ministerio de Ciencia e Innovación; SAF 2004/0416 and SAF 2007/60038), the Comunidad de Madrid (S/ SAL0261/2006), and Red Española de Esclerosis Múltiple (REEM). F. Correa received a fellowship from the Comunidad Autónoma de Madrid. M. Gauberti is a recipient of a PhD fellowship from the Conseil Régional de Basse-Normandie and the Institut national de la santé et de la recherche médicale (INSERM). F. Docagne is contracted through the financial support of the Conseil Régional de Basse-Normandie.

The authors have no financial conflict of interest.

Submitted: 8 September 2010
Accepted: 11 April 2011

REFERENCES

Arai, K., and E.H. Lo. 2009. Experimental models for analysis of oligodendrocyte pathophysiology in stroke. *Exp Transl Stroke Med*. 1:6. doi:10.1186/2040-7378-1-6

Baltan, S. 2009. Ischemic injury to white matter: an age-dependent process. *Neuroscientist*. 15:126–133. doi:10.1177/1073858408324788

Baranes, D., D. Lederfein, Y.Y. Huang, M. Chen, C.H. Bailey, and E.R. Kandel. 1998. Tissue plasminogen activator contributes to the late phase of LTP and to synaptic growth in the hippocampal mossy fiber pathway. *Neuron*. 21:813–825. doi:10.1016/S0896-6273(00)80597-8

Baron, A., A. Montagne, F. Cassé, S. Launay, E. Maubert, C. Ali, and D. Vivien. 2010. NR2D-containing NMDA receptors mediate tissue plasminogen activator-promoted neuronal excitotoxicity. *Cell Death Differ.* 17:860–871. doi:10.1038/cdd.2009.172

Baud, O., J. Li, Y. Zhang, R.L. Neve, J.J. Volpe, and P.A. Rosenberg. 2004. Nitric oxide-induced cell death in developing oligodendrocytes is associated with mitochondrial dysfunction and apoptosis-inducing factor translocation. *Eur. J. Neurosci.* 20:1713–1726. doi:10.1111/j.1460-9568.2004.03616.x

Benchenane, K., J.P. López-Atalaya, M. Fernández-Monreal, O. Touzani, and D. Vivien. 2004. Equivocal roles of tissue-type plasminogen activator in stroke-induced injury. *Trends Neurosci.* 27:155–160. doi:10.1016/j.tins.2003.12.011

Benchenane, K., V. Berezowski, M. Fernández-Monreal, J. Brillault, S. Valable, M.P. Dehouck, R. Cecchelli, D. Vivien, O. Touzani, and C. Ali. 2005. Oxygen glucose deprivation switches the transport of tPA across the blood-brain barrier from an LRP-dependent to an increased LRP-independent process. *Stroke*. 36:1065–1070. doi:10.1161/01.STR.0000163050.39122.4f

Butts, B.D., C. Houde, and H. Mehmet. 2008. Maturation-dependent sensitivity of oligodendrocyte lineage cells to apoptosis: implications for normal development and disease. *Cell Death Differ.* 15:1178–1186. doi:10.1038/cdd.2008.70

Carmeliet, P., L. Schoonjans, L. Kieckens, B. Ream, J. Degen, R. Bronson, R. De Vos, J.J. van den Oord, D. Collen, and R.C. Mulligan. 1994. Physiological consequences of loss of plasminogen activator gene function in mice. *Nature*. 368:419–424. doi:10.1038/368419a0

Chen, Z.L., and S. Strickland. 1997. Neuronal death in the hippocampus is promoted by plasmin-catalyzed degradation of laminin. *Cell*. 91:917–925. doi:10.1016/S0092-8674(00)80483-3

Correa, F., L. Mestre, F. Docagne, and C. Guaza. 2005. Activation of cannabinoid CB2 receptor negatively regulates IL-12p40 production in murine macrophages: role of IL-10 and ERK1/2 kinase signaling. *Br. J. Pharmacol.* 145:441–448. doi:10.1038/sj.bjp.0706215

Declerck, P.J., M. Verstreken, and D. Collen. 1995. Immunoassay of murine t-PA, u-PA and PAI-1 using monoclonal antibodies raised in gene-inactivated mice. *Thromb. Haemost.* 74:1305–1309.

Dewar, D., P. Yam, and J. McCulloch. 1999. Drug development for stroke: importance of protecting cerebral white matter. *Eur. J. Pharmacol.* 375:41–50. doi:10.1016/S0014-2999(99)00280-0

Docagne, F., O. Nicole, H.H. Marti, E.T. MacKenzie, A. Buisson, and D. Vivien. 1999. Transforming growth factor-beta1 as a regulator of the serpins/t-PA axis in cerebral ischemia. *FASEB J.* 13:1315–1324.

Flavin, M.P., G. Zhao, and L.T. Ho. 2000. Microglial tissue plasminogen activator (tPA) triggers neuronal apoptosis in vitro. *Glia*. 29:347–354. doi:10.1002/(SICI)1098-1136(20000215)29:4<347::AID-GLIA5>3.0.CO;2-8

Frey, U., M. Müller, and D. Kuhl. 1996. A different form of long-lasting potentiation revealed in tissue plasminogen activator mutant mice. *J. Neurosci.* 16:2057–2063.

Gerstner, B., C. Bührer, C. Rheinländer, O. Polley, A. Schüller, M. Berns, M. Obladen, and U. Felderhoff-Mueser. 2006. Maturation-dependent oligodendrocyte apoptosis caused by hyperoxia. *J. Neurosci. Res.* 84:306–315. doi:10.1002/jnr.20880

Hennebert, O., S. Marret, P. Carmeliet, P. Gressens, A. Laquerrière, and P. Leroux. 2004. Role of tissue-derived plasminogen activator (t-PA) in an excitotoxic mouse model of neonatal white matter lesions. *J. Neuropathol. Exp. Neurol.* 63:53–63.

Henson, E.S., and S.B. Gibson. 2006. Surviving cell death through epidermal growth factor (EGF) signal transduction pathways: implications for cancer therapy. *Cell. Signal.* 18:2089–2097. doi:10.1016/j.cellsig.2006.05.015

Ho, P.W., D.C. Reutens, T.G. Phan, P.M. Wright, R. Markus, I. Indra, D. Young, and G.A. Donnan. 2005. Is white matter involved in patients entered into typical trials of neuroprotection? *Stroke*. 36:2742–2744. doi:10.1161/01.STR.0000189748.52500.a7

Hurtado, M., J.J. Lozano, E. Castellanos, L.A. López-Fernández, K. Harshman, C. Martínez-A, A.R. Ortiz, T.M. Thomson, and R. Paciucci. 2007. Activation of the epidermal growth factor signalling pathway by tissue plasminogen activator in pancreas cancer cells. *Gut*. 56:1266–1274. doi:10.1136/gut.2006.097188

Husain, J., and B.H. Juurlink. 1995. Oligodendroglial precursor cell susceptibility to hypoxia is related to poor ability to cope with reactive oxygen species. *Brain Res.* 698:86–94. doi:10.1016/0006-8993(95)00832-B

Kilic, E., M. Bähr, and D.M. Hermann. 2001. Effects of recombinant tissue plasminogen activator after intraluminal thread occlusion in mice: role of hemodynamic alterations. *Stroke*. 32:2641–2647. doi:10.1161/hs1101.097381

Kim, Y.H., J.H. Park, S.H. Hong, and J.Y. Koh. 1999. Nonproteolytic neuroprotection by human recombinant tissue plasminogen activator. *Science*. 284:647–650. doi:10.1126/science.284.5414.647

Lansberg, M.G., E. Bluhmki, and V.N. Thijs. 2009. Efficacy and safety of tissue plasminogen activator 3 to 4.5 hours after acute ischemic stroke: a meta-analysis. *Stroke*. 40:2438–2441. doi:10.1161/STROKEAHA.109.552547

Lee, H.Y., I.Y. Hwang, H. Im, J.Y. Koh, and Y.H. Kim. 2007. Non-proteolytic neurotrophic effects of tissue plasminogen activator on cultured mouse cerebrocortical neurons. *J. Neurochem.* 101:1236–1247. doi:10.1111/j.1471-4159.2007.04417.x

Liot, G., K. Benchenane, F. Léveillé, J.P. López-Atalaya, M. Fernández-Monreal, A. Ruocco, E.T. Mackenzie, A. Buisson, C. Ali, and D. Vivien. 2004. 2,7-Bis-(4-amidinobenzylidene)-cycloheptan-1-one dihydrochloride, tPA stop, prevents tPA-enhanced excitotoxicity both in vitro and in vivo. *J. Cereb. Blood Flow Metab.* 24:1153–1159. doi:10.1097/01.WCB.0000134476.93809.75

Liot, G., B.D. Roussel, N. Lebeurrier, K. Benchenane, J.P. López-Atalaya, D. Vivien, and C. Ali. 2006. Tissue-type plasminogen activator rescues neurones from serum deprivation-induced apoptosis through a mechanism independent of its proteolytic activity. *J. Neurochem.* 98:1458–1464. doi:10.1111/j.1471-4159.2006.03982.x

Liu, D., T. Cheng, H. Guo, J.A. Fernández, J.H. Griffin, X. Song, and B.V. Zlokovic. 2004. Tissue plasminogen activator neurovascular toxicity is controlled by activated protein C. *Nat. Med.* 10:1379–1383. doi:10.1038/nm1122

Lu, W., M. Bhasin, and S.E. Tsirka. 2002. Involvement of tissue plasminogen activator in onset and effector phases of experimental allergic encephalomyelitis. *J. Neurosci.* 22:10781–10789.

Matute, C., M. Domercq, and M.V. Sánchez-Gómez. 2006. Glutamate-mediated glial injury: mechanisms and clinical importance. *Glia*. 53:212–224. doi:10.1002/glia.20275

Minor, K., J. Phillips, and N.W. Seeds. 2009. Tissue plasminogen activator promotes axonal outgrowth on CNS myelin after conditioned injury. *J. Neurochem.* 109:706–715. doi:10.1111/j.1471-4159.2009.05977.x

Molina-Holgado, E., J.M. Vela, A. Arévalo-Martín, G. Almazán, F. Molina-Holgado, J. Borrell, and C. Guaza. 2002. Cannabinoids promote oligodendrocyte progenitor survival: involvement of cannabinoid receptors and phosphatidylinositol-3 kinase/Akt signaling. *J. Neurosci.* 22:9742–9753.

Nagai, N., M. De Mol, H.R. Lijnen, P. Carmeliet, and D. Collen. 1999. Role of plasminogen system components in focal cerebral ischemic infarction: a gene targeting and gene transfer study in mice. *Circulation*. 99:2440–2444.

Ness, J.K., M.J. Romanko, R.P. Rothstein, T.L. Wood, and S.W. Levison. 2001. Perinatal hypoxia-ischemia induces apoptotic and excitotoxic death of periventricular white matter oligodendrocyte progenitors. *Dev. Neurosci*. 23:203–208. doi:10.1159/000046144

Nicole, O., F. Docagne, C. Ali, I. Margaill, P. Carmeliet, E.T. MacKenzie, D. Vivien, and A. Buisson. 2001. The proteolytic activity of tissue-plasminogen activator enhances NMDA receptor-mediated signaling. *Nat. Med*. 7:59–64. doi:10.1038/83358

O'Collins, V.E., M.R. Macleod, G.A. Donnan, L.L. Horky, B.H. van der Worp, and D.W. Howells. 2006. 1,026 experimental treatments in acute stroke. *Ann. Neurol.* 59:467–477. doi:10.1002/ana.20741

Ortiz-Zapater, E., S. Peiró, O. Roda, J.M. Corominas, S. Aguilar, C. Ampurdanés, F.X. Real, and P. Navarro. 2007. Tissue plasminogen activator induces pancreatic cancer cell proliferation by a non-catalytic mechanism that requires extracellular signal-regulated kinase 1/2 activation through epidermal growth factor receptor and annexin A2. *Am. J. Pathol.* 170:1573–1584. doi:10.2353/ajpath.2007.060850

Pantoni, L., J.H. Garcia, and J.A. Gutierrez. 1996. Cerebral white matter is highly vulnerable to ischemia. *Stroke*. 27:1641–1646, discussion :1647.

Raghupathi, R. 2004. Cell death mechanisms following traumatic brain injury. *Brain Pathol.* 14:215–222. doi:10.1111/j.1750-3639.2004.tb00056.x

Rogove, A.D., and S.E. Tsirka. 1998. Neurotoxic responses by microglia elicited by excitotoxic injury in the mouse hippocampus. *Curr. Biol.* 8:19–25. doi:10.1016/S0960-9822(98)70016-8

Rojas, M., S. Yao, and Y.Z. Lin. 1996. Controlling epidermal growth factor (EGF)-stimulated Ras activation in intact cells by a cell-permeable peptide mimicking phosphorylated EGF receptor. *J. Biol. Chem.* 271:27456–27461. doi:10.1074/jbc.271.44.27456

Roussel, B.D., R. Macrez, A. Jullienne, V. Agin, E. Maubert, L. Dauphinot, M.C. Potier, L. Plawinski, H. Castel, Y. Hommet, et al. 2009. Age and albumin D site-binding protein control tissue plasminogen activator levels: neurotoxic impact. *Brain*. 132:2219–2230. doi:10.1093/brain/awp162

Salter, M.G., and R. Fern. 2005. NMDA receptors are expressed in developing oligodendrocyte processes and mediate injury. *Nature*. 438:1167–1171. doi:10.1038/nature04301

Sánchez-Gómez, M.V., E. Alberdi, G. Ibarretxe, I. Torre, and C. Matute. 2003. Caspase-dependent and caspase-independent oligodendrocyte death mediated by AMPA and kainate receptors. *J. Neurosci*. 23:9519–9528.

Shapira, S., M. Sapir, A. Wengier, E. Grauer, and T. Kadar. 2002. Aging has a complex effect on a rat model of ischemic stroke. *Brain Res.* 925:148–158. doi:10.1016/S0006-8993(01)03270-X

Shibata, M., S. Hisahara, H. Hara, T. Yamawaki, Y. Fukuuchi, J. Yuan, H. Okano, and M. Miura. 2000. Caspases determine the vulnerability of oligodendrocytes in the ischemic brain. *J. Clin. Invest.* 106:643–653. doi:10.1172/JCI10203

Siao, C.J., and S.E. Tsirka. 2002. Tissue plasminogen activator mediates microglial activation via its finger domain through annexin II. *J. Neurosci.* 22:3352–3358.

Sozmen, E.G., A. Kolekar, L.A. Havton, and S.T. Carmichael. 2009. A white matter stroke model in the mouse: axonal damage, progenitor responses and MRI correlates. *J. Neurosci. Methods*. 180:261–272. doi:10.1016/j.jneumeth.2009.03.017

Thiyagarajan, M., J.A. Fernández, S.M. Lane, J.H. Griffin, and B.V. Zlokovic. 2008. Activated protein C promotes neovascularization and neurogenesis in postischemic brain via protease-activated receptor 1. *J. Neurosci*. 28:12788–12797. doi:10.1523/JNEUROSCI.3485-08.2008

Vemuri, G.S., and F.A. McMorris. 1996. Oligodendrocytes and their precursors require phosphatidylinositol 3-kinase signaling for survival. *Development*. 122:2529–2537.

Wang, Y.F., S.E. Tsirka, S. Strickland, P.E. Stieg, S.G. Soriano, and S.A. Lipton. 1998. Tissue plasminogen activator (tPA) increases neuronal damage after focal cerebral ischemia in wild-type and tPA-deficient mice. *Nat. Med*. 4:228–231. doi:10.1038/nm0298-228

Wasserman, J.K., and L.C. Schlichter. 2008. White matter injury in young and aged rats after intracerebral hemorrhage. *Exp. Neurol.* 214:266–275. doi:10.1016/j.expneurol.2008.08.010

Yepes, M., B.D. Roussel, C. Ali, and D. Vivien. 2009. Tissue-type plasminogen activator in the ischemic brain: more than a thrombolytic. *Trends Neurosci.* 32:48–55. doi:10.1016/j.tins.2008.09.006

Young, A.R., C. Ali, A. Duretête, and D. Vivien. 2007. Neuroprotection and stroke: time for a compromise. *J. Neurochem.* 103:1302–1309. doi:10.1111/j.1471-4159.2007.04866.x